

An Overview of Ground-based Radar and Optical Measurements Utilized by the NASA Orbital Debris Program Office

**Alyssa Manis⁽¹⁾, Jessica A. Arnold⁽²⁾, James Murray⁽³⁾, Brent Buckalew⁽²⁾, Corbin Cruz⁽²⁾,
and Mark Matney⁽¹⁾**

⁽¹⁾ NASA Orbital Debris Program Office, NASA Johnson Space Center, Mail Code XI5-9E, 2101 NASA Parkway, Houston, TX 77058, USA; alyssa.p.manis@nasa.gov; mark.matney-1@nasa.gov

⁽²⁾ Jacobs, NASA Orbital Debris Program Office, NASA Johnson Space Center, Mail Code XI5-9E, 2101 NASA Parkway, Houston, TX 77058, USA; jessica.a.arnold@nasa.gov; brent.a.buckalew@nasa.gov; corbin.l.cruz@nasa.gov

⁽³⁾ Tomorrow.io, 9 Channel Center St., 7th Floor, Boston, MA 02210, USA, USA; james.murray@tomorrow.io

Abstract

For over 30 years, the NASA Orbital Debris Program Office (ODPO) has led the characterization of orbital debris (OD) too small to be tracked by the U.S. Space Surveillance Network (SSN), yet which may pose the greatest threat to human spaceflight and robotic missions. Measurements from specialized sensors, including ground-based radars and telescopes capable of detecting smaller objects, provide the foundation for developing statistical models to describe the current state and future evolution of the OD environment from low Earth orbit (LEO) to geosynchronous orbit (GEO). Since 1990, the ODPO has partnered with the U.S. Department of Defense and the Massachusetts Institute of Technology Lincoln Laboratory (MIT/LL) to collect data using the Haystack Ultrawideband Satellite Imaging Radar (HUSIR) – formerly Haystack – to characterize OD in LEO with a sensitivity of approximately 5 mm at 1000 km altitude. In addition, since 1993, the Goldstone Orbital Debris Radar, operated by NASA’s Jet Propulsion Laboratory, has provided data on OD as small as approximately 2-3 mm for altitudes below 1000 km, some of the most sensitive ground-based measurements achievable at these altitudes. Recently, collaborations with the 18th Space Control Squadron of the U.S. Space Force have also provided the ODPO with special datasets from the Space Fence to extend coverage below the historical SSN limit of 10 cm and to characterize individual breakup events in LEO. For GEO altitudes, the Eugene Stansbery Meter Class Autonomous Telescope (ES-MCAT), a joint NASA-Air Force Research Laboratory project that reached full operational capability in 2021, collects data on debris smaller than 1 m and provides coverage of debris in historically under-sampled high-altitude orbital regimes. This paper summarizes the radar and optical sensors utilized by the ODPO, their unique capabilities, and recent datasets and applications for statistical sampling of the dynamic OD environment.

1 Background

The NASA Orbital Debris Program Office (ODPO) is an international leader in developing empirical models of the orbital debris (OD) environment, focusing on populations that are too small to be tracked by the U.S. Space Surveillance Network (SSN) but large enough to threaten human spaceflight and robotic missions. While larger objects are tracked to obtain precise orbit information, the ODPO utilizes ground-based sensors and *in situ* sources to statistically sample OD populations to develop a broad understanding of their number, size, and general orbital regimes.

Figure 1 shows notional coverage in altitude and size for different data sources utilized by the ODPO, covering altitudes from low Earth orbit (LEO) to geosynchronous orbit (GEO). The SSN provides data on

trackable objects down to approximately 10 cm in LEO and approximately 1 m in GEO. Below those sizes, the ODPO relies on specialized sensors capable of detecting objects at smaller size ranges.

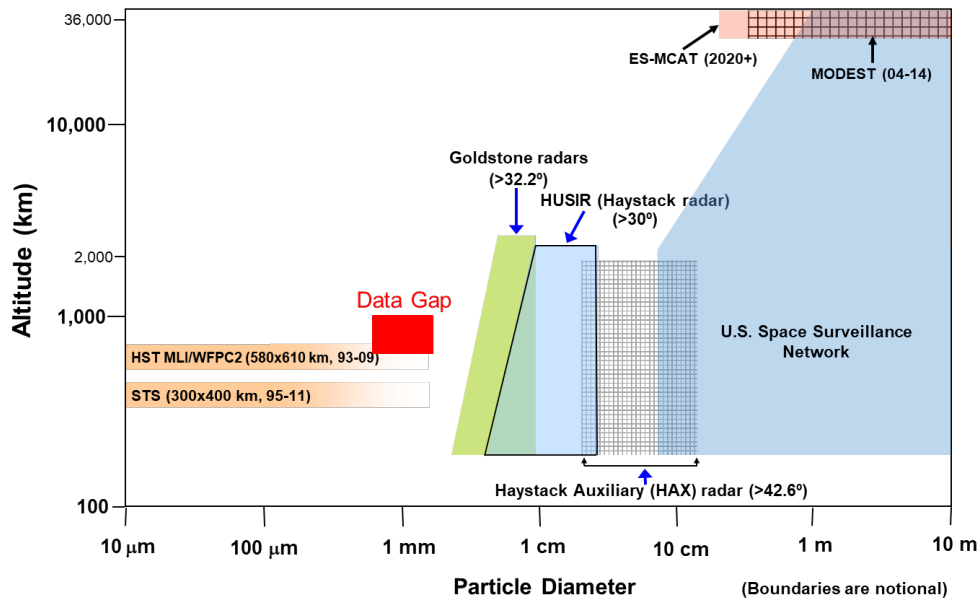


Fig 1. Notional altitude and size coverage of measurement data utilized by the ODPO. Both axes are on a logarithmic scale to better capture the range in altitudes. Goldstone notional coverage is representative of its legacy pointing configuration.

Ground-based radar measurements are the primary source of data on small debris from a few millimeters up to the SSN sensitivity limit. The Haystack Ultrawideband Satellite Imaging Radar (HUSIR), operated by the Massachusetts Institute of Technology’s Lincoln Laboratory (MIT/LL), provides data on debris with nominal sizes down to approximately 5 mm at altitudes less than 1000 km and 2 to 3 cm throughout LEO. The Goldstone Orbital Debris Radar (Goldstone), operated by NASA’s Jet Propulsion Laboratory (JPL), extends this coverage down to approximately 2 mm at 1000 km and below. Historically, the ODPO also received data on debris down to a few centimeters from the Haystack Auxiliary Radar (HAX), also operated by MIT/LL. As of U.S. Government fiscal year (FY) 2021, the ODPO no longer receives data from HAX, with preference given to obtaining data from the more sensitive HUSIR.

At GEO altitudes, ground-based optical measurements provide data on debris below the SSN size threshold. For a decade, the Michigan Orbital Debris Survey Telescope (MODEST) was the primary source for GEO debris detections down to approximately 30 cm. Since 2020, the ODPO has utilized the Eugene Stansbery Meter Class Autonomous Telescope (ES-MCAT), a joint NASA-Air Force Research Laboratory project, to survey debris in GEO down to a few tens of centimeters.

Estimates on OD orbits and sizes obtained from these specialized radar and optical measurements are critical for developing, updating, and validating OD environment models, in particular the NASA Orbital Debris Engineering Model (ORDEM) [1, 2]. This model is used primarily by satellite designers and operators to compute the mission risk to their vehicles from OD impacts. These measurements are also a valuable tool for understanding the accuracy of breakup models such as the NASA Standard Satellite Breakup Model (SSBM) [3].

This paper gives an overview of HUSIR, Goldstone, and ES-MCAT, including their unique capabilities and sample measurements. Special observations and applications to OD modeling are also summarized.

2 Radar Sensors

2.1 Radar System Overview

Since 1990, MIT/LL has collected radar measurements for the ODPO under agreements with the U.S. Department of Defense [4]. The Haystack radar, renamed HUSIR after upgrades and a return to operations in 2014, is in Westford, Massachusetts, and has been the ODPO's primary source of OD radar data in LEO below the SSN size threshold. Since FY2020, the ODPO nominally receives 500 hours of data from MIT/LL each year.

Goldstone is part of the Goldstone Deep Space Communications Complex in the Mojave Desert near Barstow, California. Since 1993, Goldstone has provided the ODPO data on OD as small as approximately 2 mm in LEO. Its sensitivity makes it a valuable asset to bridge the data gap in the millimeter-size range between the lower limit of HUSIR sensitivity and the upper limit of data available from *in situ* sources. As of FY2023, the ODPO receives approximately 290 hours of data from Goldstone each year.

HUSIR and Goldstone are shown in Fig. 2, and their precise locations are given in Table 1. For OD measurements, both radars operate in a beampark or staring mode, fixed at selected elevation and azimuth angles, and detecting debris that pass through the radar beam. They transmit right-hand circularly polarized waveforms, receiving both right- and left-hand circularly polarized returns, referred to as the orthogonal polarization (OP) and principal polarization (PP), respectively. HUSIR transmits a pulsed continuous wave (CW) waveform centered at 10.1 GHz. Goldstone transmits a pulsed linear frequency modulated “chirp” waveform centered at 8.56 GHz, with a new continuous sawtooth waveform in development [5]. A summary of their nominal operating parameters is given in Table 2; here, sensitivity is defined as the single pulse signal-to-noise ratio (SNR) for an object with a radar cross-section (RCS) of one square meter at 1000 km slant range.



Fig. 2. (Left) HUSIR is the large radome to the left of the image, and HAX is the smaller radome to the right. (Credit: Reprinted with permission Courtesy of MIT Lincoln Laboratory, Lexington, Massachusetts) (Right) The Goldstone 70 m transmit antenna. (Credit: NASA/JPL-Caltech)

Table 1. HUSIR and Goldstone Location with Respect to the 1984 World Geodetic System (WGS 84) Earth Model

| Radar | Latitude | Longitude | Elevation |
|-------------------------|--------------|---------------|-----------|
| HUSIR | 42.623287° N | 288.511846° E | 115.69 m |
| Goldstone (transmitter) | 35.425901° N | 243.110464° E | 1001.39 m |

Table 2. Nominal Operating Parameters for HUSIR and Goldstone

| Operating Parameter | HUSIR | Goldstone |
|--|--------|---------------------------------------|
| Peak Transmit Power (kW) | 250 | 440 |
| Transmit Frequency (GHz) | 10.1 | 8.56 |
| Wavelength (cm) | 3.0 | 3.5 |
| Antenna Diameter (m) | 36.6 | 70 (transmitter) 34 (receiver) |
| Half Power Beamwidth (deg) | 0.058 | 0.03 (transmitter) 0.06 (receiver) |
| Sensitivity (dB) | 59.2 | 67.7 |
| Intermediate Frequency Bandwidth (MHz) | 1.25 | 1.5 |
| Pulse (chirp) Duration (ms) | 1.6384 | 2.9 |
| Pulse (chirp) Bandwidth (kHz) | N/A | 300 |
| Pulse Repetition Frequency (Hz) | 60 | 55.6 |

HUSIR is a monostatic radar that uses a single 36.6 m-diameter Cassegrain reflector for both the transmit and receive antenna. Typical pointing geometries employed by the ODPO are 75° elevation, due East (75E); 20° elevation, due South (20S); and 10° elevation, due South (10S). By staring just off-zenith, the 75E staring geometry allows the radar to measure Doppler shifts that give meaningful orbital information for orbital inclinations between approximately 40° and 140° using a circular orbit approximation. In the 75E staring geometry, HUSIR samples between 392 km and 2166 km altitude. The 75E staring geometry comprises approximately two-thirds of the total observation time spent collecting OD radar data from HUSIR each year, with the remaining third of observation time split approximately evenly between the 10S and 20S geometries. The south-staring geometries suffer from reduced sensitivity due to increased atmospheric attenuation and longer path length for a given altitude; however, they allow HUSIR to view lower orbital inclinations down to approximately 20°. HUSIR has historically used a waveform centered at 10 GHz for debris measurements. Due to increasingly prevalent radio frequency interference (RFI) at 10 GHz, MIT/LL developed a new CW waveform with a center frequency of 10.1 GHz in 2020. The 10.1 GHz waveform has been used exclusively since 01 October 2021 and has proven highly effective, with no RFI contamination seen in the 10.1 GHz data in calendar year (CY) 2021 or CY2022.

The Goldstone radar is a bistatic system; it uses a 70 m- and 34 m-diameter Cassegrain reflector for the transmit and receive antennas, respectively. The Deep Space Station (DSS)-14 antenna is used as a transmitter. Before 2018, DSS-15 was used as a receiver, providing a relatively short baseline of 500 m between transmitter and receiver that allowed the beams to overlap all of LEO with a single pointing. In early 2018, DSS-15 was decommissioned and replaced with DSS-25 and DSS-26 of the Deep Space Network Apollo Cluster. The current configuration has a large, approximately 10 km baseline, so that the antenna beams overlap for a small part of LEO for a given pointing. To compensate for this change, the ODPO developed a new observation strategy for Goldstone to optimize coverage over altitudes of interest. Details on the new pointing plan can be found in [6]. With the transmit antenna using the 75E pointing, four different pointings of the receive antenna (termed A, B, C, and D) are used to efficiently cover 700 km to 1000 km altitude without significant sensitivity loss relative to the historical configuration. In fact, the new pointing plan has provided improved sensitivity over the altitude range of interest. With the legacy configuration, Goldstone's minimum completeness size was approximately 3 mm at 1000 km altitude. With a new minimum completeness size of approximately 2.2 mm at

1000 km altitude, Goldstone now provides some of the most sensitive measurements of OD in LEO made with terrestrial radar, to date. In addition to the new observation plan, the ODPO is actively working with JPL to develop a strategy to sample OD in medium Earth orbit (MEO), which would help fill a gap in measurements at these higher altitudes.

2.2 Radar Measurements

Statistical radar measurements are usually evaluated on an annual basis, which allows for observing general trends in the environment as well as effects from specific events. The fundamental measurements made by the radar are range, range-rate (or Doppler velocity), and received power from which RCS can be calculated. These direct measurements are used to estimate quantities of interest for each detection, including altitude, inclination, and size.

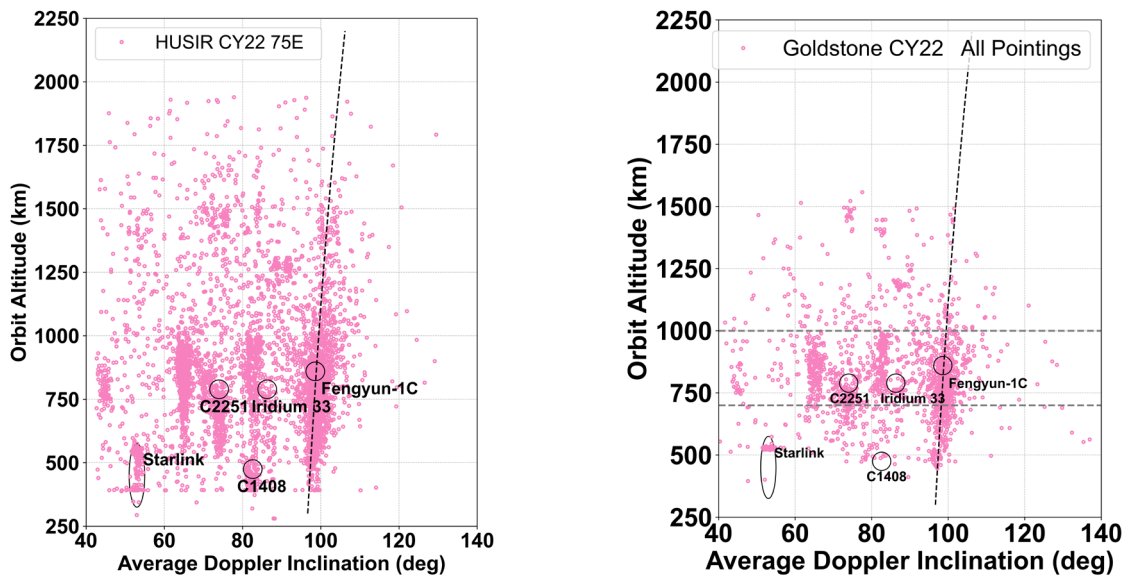


Fig. 3. Orbit altitude versus average Doppler inclination for HUSIR (left) and Goldstone (right) 75E detections in CY2022. Goldstone detections are from all four pointings. Notable breakups and the region of Starlink detections are circled. The dashed black curve indicates the sun-synchronous condition for circular orbits.

Because of the short arc of an object's path through the beam when operating in beampark mode, obtaining full orbital information with sufficient accuracy to construct precise orbits is not possible. An object's range and range-rate measurements, however, can be converted to orbit altitude and Doppler inclination by assuming a circular orbit. The orbit altitude versus average Doppler inclination from HUSIR and Goldstone detections in CY 2022 are shown in Fig. 3. In this view, several debris families are apparent in both datasets. The largest of these is the sun-synchronous family of orbits clustered around the dashed black curve indicating the sun-synchronous inclinations for circular orbits. Several notable on-orbit fragmentation events are designated with black circles, namely the Fengyun-1C anti-satellite (ASAT) test of 2007, the accidental collision of Iridium 33 and Cosmos 2251 (C2251) in 2009, and the Cosmos 1408 (C1408) ASAT test of 2021. The centers of the circles correspond to the altitude and inclination of the parent body at the time of the event. In addition, detections associated with the Starlink constellation at approximately 53° inclination are identified by the black ellipse. For Goldstone, there are fewer detections outside the 700-1000 km altitude band of interest, indicated by the horizontal black dashed lines, due to the reduced sensitivity at those altitudes with the new pointing plan.

Another fundamental measurement obtained from the radar is RCS. This is converted to an object size using the NASA size estimation model (SEM), which relates RCS to an object’s physical size through a polynomial fit to laboratory RCS measurements of 39 representative debris objects over many orientations and at a range of frequencies [7]. Figure 4 shows the cumulative flux as a function of SEM-derived size from HUSIR 75E and the Goldstone Pointing A in CY2021 and CY2023 (through June). The orbit altitude is limited to 660.3–806.4 km for data from both sensors, which is the main beam overlap of the Goldstone Pointing A. The higher sensitivity of Goldstone compared to HUSIR is evident in Fig. 4, with Goldstone extending the size coverage from HUSIR down to approximately 2 mm.

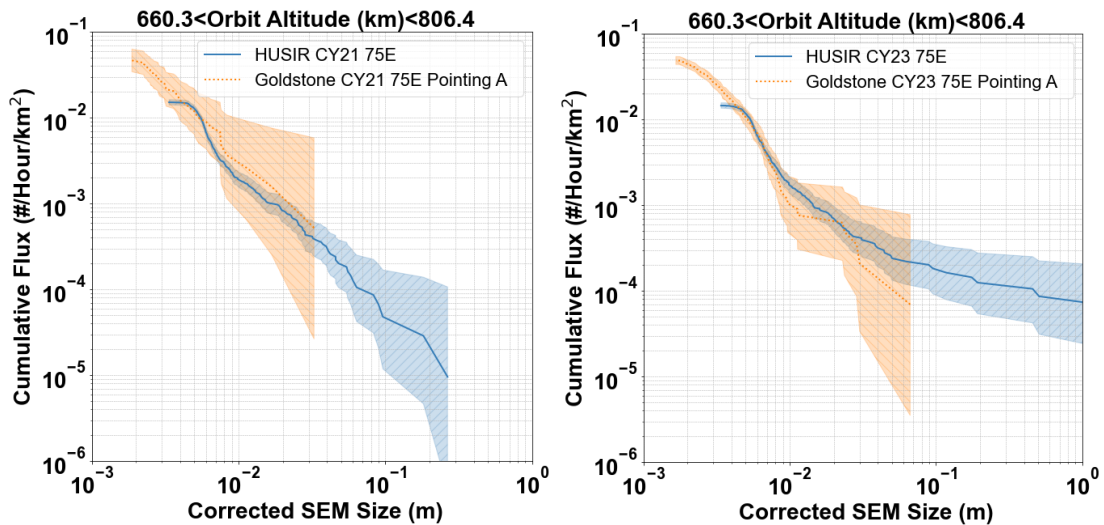


Fig. 4. Cumulative flux versus SEM size for HUSIR and Goldstone in CY2021 (left) and CY2023 (through June, right). Shaded regions represent the 2σ Poisson uncertainties.

2.3 Special Observations

In addition to regular statistical sampling of the OD environment, HUSIR and Goldstone have also been used for rapid-response breakup support to characterize fragments from breakup events. Most recently, after the Russian Federation conducted a direct-ascent ASAT test against C1408 (International Designator 1982-092A, Catalog Number 13552) on 15 November 2021, the ODPO coordinated with MIT/LL and JPL to perform a special observation campaign of the small C1408 fragments beginning the day after the event through 11 December 2021. In addition, MIT/LL, in coordination with the 18th Space Control Squadron (18 SPCS) of the U.S. Space Force (USSF), shared a unique dataset consisting of the first two passes of the fragment cloud over the Space Fence on Kwajalein Atoll in the Marshall Islands. The data from all sensors was processed similarly and compared to model predictions for the cumulative size distribution of C1408 fragments based on the NASA SSBM. As shown in Fig. 5, the SSBM prediction matches the distributions from the special datasets extremely well across all size ranges. This good agreement serves to validate the C1408 model predictions from the SSBM; therefore, the modeled C1408 debris cloud was subsequently incorporated into the updated ORDEM version 3.2 [8]. Additional analysis of the C1408 detections from HUSIR and Goldstone is presented in [9].

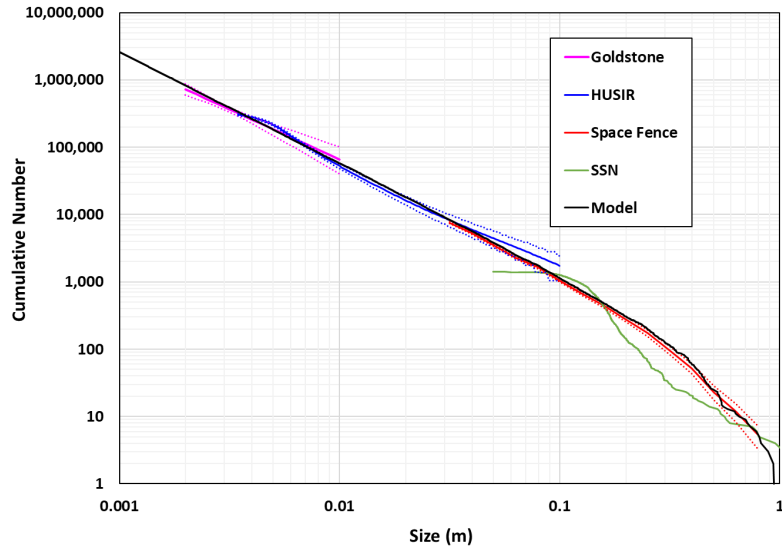


Fig. 5. The cumulative size distribution of C1408 fragments based on special observation campaigns from Goldstone, HUSIR, and the Space Fence. Dotted curves represent the measurement uncertainties, and the black curve shows the NASA SSBM prediction.

3 Optical Sensors

3.1 ES-MCAT Overview

The ES-MCAT observatory (shown in Fig. 6) is located on the USSF base (Space Launch Delta 45, Detachment 2) near the Ascension Auxiliary Airfield on Ascension Island. It is positioned at $7^{\circ} 58' S$, $14^{\circ} 4' W$ and 350' elevation. ES-MCAT was designed to operate fully autonomously by the ODPO because of its remote location [10]. ES-MCAT is a 1.3-m, f/4, DFM Engineering fast-tracking optical telescope paired with an Observa-Dome fast-tracking dome to accommodate tracking debris at all orbital altitudes. It is equipped with a 4096 by 4096-pixel charge-coupled device camera and has a field of view (FOV) of 0.68° by 0.68° (0.96° diagonal). Nominal GEO survey observations with ES-MCAT use the Sloan Digital Sky Survey (SDSS) r' or g' filters with a standard exposure time of 10 s, and detections are counted if the object appears in at least four frames, up to a maximum of seven. Additional details on the GEO survey observation strategy employed by ES-MCAT are given in [11].



Fig. 6. ES-MCAT, located on Ascension Island. (Credit: Ben Hanna)

ES-MCAT achieved first light in 2015 and reached full operational capability in 2021. Its primary observation goal is to extend GEO coverage to smaller (fainter) OD. Its near-equatorial latitude ensures that low-inclination LEO, GEO, and GEO transfer orbit (GTO) target orbits pass overhead, so that all orbit inclinations are viewable. As a result, its location is ideal for statistically sampling historically under-sampled LEO, MEO, GEO, and GTO orbital regions. Unlike previous sensors utilized by the ODPO, ES-MCAT is a dedicated NASA sensor and can also be tasked for rapid-response breakup support and special observations of targets of interest as needed. Collaborations are actively underway between the ODPO and the USSF to make ES-MCAT a contributing sensor to the SSN.

ES-MCAT recently completed its first two-year survey of the GEO environment in February 2022 [11]. Because the primary mirror degraded due to COVID-19 travel restrictions that prevented regular cleaning, it was recoated in 2022 and reinstalled in January 2023. The second GEO survey is underway and is planned to continue through 2025. With the newly recoated mirror, the limiting magnitude is estimated at approximately 22.

3.2 Optical Measurements

The direct telescope measurements of right ascension, declination, and magnitude are used to estimate the desired orbit and size information of debris objects. Since the orbital arc of ES-MCAT GEO survey detections is a short 2–4 min, a circular orbit is assumed to estimate orbital elements. Objects are correlated to the publicly available SSN catalog. Detected objects found in the catalog are termed correlated targets (CTs), while objects not correlated to cataloged objects are termed uncorrelated targets (UCTs). Detections are also assigned an expectation value (EVAL), which is a measure of the probability of detecting an object in a specific orbit for a given FOV and time, based on composite coverage for the full observing period of the survey. An object's EVAL is used to determine its weight ($1/\text{EVAL}$); this statistically accounts for multiple detections of the same object as well as objects sampled from a population which is, on average, undetected or under-sampled.

An object's inclination (INC) and right ascension of the ascending node (RAAN) are not significantly affected by the circular orbit assumption, so these parameters are used to provide information on an object's orbit characteristics to aid in identifying those that are most likely GEO debris. Uncontrolled objects in GEO naturally precess in INC and RAAN space due to effects from the Earth's oblateness and the gravity of the Sun and Moon [12]. This natural precession appears as a loop in the Cartesian coordinates of $[\text{INC}\cdot\cos(\text{RAAN}), \text{INC}\cdot\sin(\text{RAAN})]$, which represents the projection of the orbit's angular momentum vector on the equatorial plane.

Figure 7 shows the detections in $[\text{INC}\cdot\cos(\text{RAAN}), \text{INC}\cdot\sin(\text{RAAN})]$ space from the first three months of ES-MCAT's ongoing second GEO survey, from 16 January 2023 through 16 April 2023, for CTs (left) and UCTs (right). Detections are color-coded by their EVAL, *e.g.*, redder colors indicate a larger EVAL (and subsequently lower weight) while bluer colors indicate a smaller EVAL (and higher weight). The outer, dashed black circle shows the primary target region of interest for GEO survey observations. Also plotted in Fig. 7 are modeled GEO intact and debris objects from ORDEM 3.2, propagated to the end of 2019 and represented by gray dots. Black dots show fragments from the 2019 breakup of a Titan Transtage (International Designator 1976-023F, Catalog Number 8751) as modeled with the NASA SSBM and propagated to the end of 2023. This modeled breakup cloud highlights the importance of regularly monitoring observation strategies and incorporating special observations as needed to ensure adequate coverage of debris populations.

The other fundamental debris measurement of size is converted from an object's absolute magnitude – calibrated to 36,000 km altitude and assuming a Lambertian phase function correction – using the NASA optical size estimation model [13]. Figure 8 shows the cumulative number (using objects' weights) as a

function of size for the UCTs and CT debris from the first (20–22) and ongoing second (23–25) GEO surveys. The NASA SSBM for explosions (EXP) is shown scaled by a factor of 8, corresponding to the number of confirmed breakups that have occurred in GEO to date [14]. The ES-MCAT detections from the first part of 2023 match the SSBM prediction very well both in terms of weighted number and slope from approximately 20 cm to 1 m. The apparent discrepancy of the ES-MCAT 2020 to 2022 detections may be a result of uncertainties in measured magnitudes and/or incompleteness of detections due to the primary mirror degradation during that time.

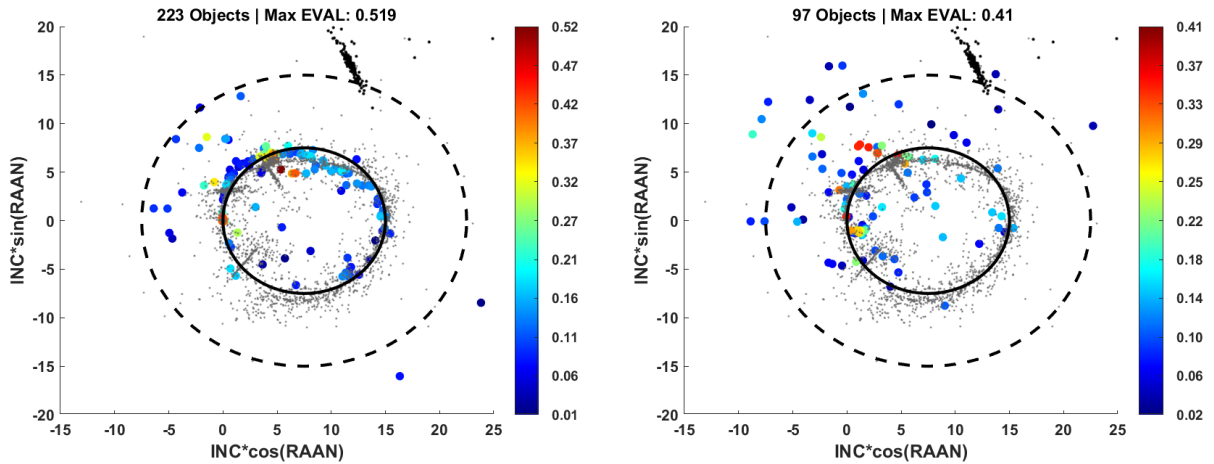


Fig. 7. CT (left) and UCT (right) detections from the ES-MCAT second GEO survey in $[INC \cdot \cos(RAAN), INC \cdot \sin(RAAN)]$ space, color-coded by the objects' EVALs. The region of interest for GEO survey observations is shown by the outer, dashed black circle. GEO objects from ORDEM 3.2 and a 2019 Titan Transtage breakup modeled using the NASA SSBM are shown by gray and black dots, respectively.

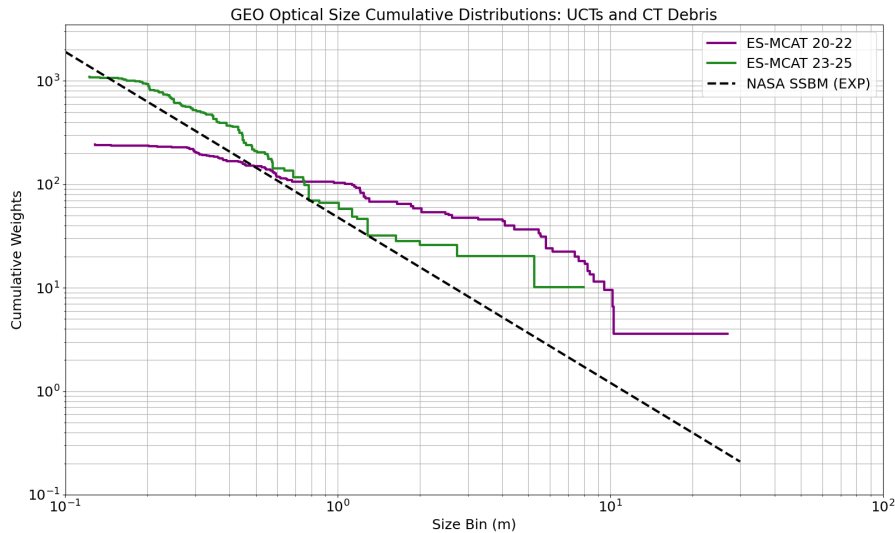


Fig. 8. Cumulative size distribution for ES-MCAT UCT and CT debris detections from the 2020 to 2022 GEO survey and the first three months of the second GEO survey. The NASA SSBM for explosions (EXP) is shown scaled by a factor of 8, corresponding to the number of confirmed breakups that have occurred in GEO to date.

4 Summary

HUSIR, Goldstone, and ES-MCAT, as well as auxiliary sensors such as the Space Fence, offer unique capabilities to survey small debris sized down to a few millimeters in LEO and a few tens of centimeters in GEO. Continued monitoring of the OD environment is essential to understand the evolution of OD populations and the interdependence of this changing environment and space activities. Regular statistical measurements capture the year-to-year trends in the overall environment as well as the dynamic effects of individual breakup events, providing timely data for updating OD environment models.

5 References

1. Manis, A., Matney, M., Vavrin, A., *et al.* "NASA Orbital Debris Engineering Model (ORDEM) 3.1: Model Process," NASA/TP-20220004345, March 2022.
2. Kennedy, T., *et al.* "NASA Orbital Debris Engineering Model (ORDEM) 3.1: Model Verification and Validation," NASA/TP-20220002309, February 2022.
3. Johnson, N.L., *et al.* NASA's New Breakup Model of EVOLVE 4.0, *Adv. Space Res.*, vol. 28, issue 9, pp. 1377-1384, 2001.
4. E.G. Stansbery, *et al.* "Characterization of the Orbital Debris Environment from Haystack radar measurements," *Adv. Space Res.*, vol. 16, issue 11, pp. 5-16, 1995.
5. Jao, J.S., Lee, *et al.* "Continuous Chirp Waveform Study from Goldstone Orbital Debris Radar Observations," to be presented at the Second International Orbital Debris Conference, Sugar Land, TX, 2023.
6. Murray, J., *et al.* "Optimizing Altitude Sampling and Sensitivity with the Goldstone Orbital Debris Radar," to be presented at the Second International Orbital Debris Conference, Sugar Land, TX, 2023.
7. Xu, Y.-L., *et al.* "A Statistical Size Estimation Model for Haystack and HAX Radar Detections," 56th International Astronautical Congress, Fukuoka, Japan, 2005.
8. NASA Orbital Debris Program Office. "Orbital Debris Engineering Model 3.2 Release," *Orbital Debris Quarterly News*, vol. 26, Issue 1, p. 5, March 2022.
9. Murray, J., *et al.* "Observations of Small Debris from the Cosmos 1408 Anti-Satellite Test using the HUSIR and Goldstone Radars," Proceedings of the 2022 AMOS Technical Conference, Wailea, Maui, HI, pp. 1833-1842, 2022.
10. Hickson, P. "OCS: A Flexible Observatory Control System for Robotic Telescopes with Application to Detection and Characterization of Orbital Debris," First International Orbital Debris Conference, Sugar Land, TX, 2019.
11. Cruz, C., *et al.* "The Completion of a Geosynchronous Earth Orbit Survey with the Eugene Stansbery-Meter Class Autonomous Telescope," to be presented at the Second International Orbital Debris Conference, Sugar Land, TX, 2023.
12. Abercromby, K.J., *et al.* "Michigan Orbital DEbris Survey Telescope Observations of the Geosynchronous Orbital Debris Environment, Observing Years: 2004 – 2006," NASA/TP-2010-216129, August 2010.
13. Barker, E.S., *et al.* "Analysis of Working Assumptions in the Determination of Populations and Size Distributions of Orbital Debris from Optical Measurements," Proceedings of the 2004 AMOS Technical Conference, Wailea, Maui, HI, pp. 225-235, 2004.
14. Anz-Meador, P.D., *et al.* "History of On-Orbit Satellite Fragmentations 16th Edition," NASA/TP-20220019160, December 2022.